Bioorganic & Medicinal Chemistry Letters 18 (2008) 4904–4906

Contents lists available at ScienceDirect

Bioorganic & Medicinal Chemistry Letters

journal homepage: www.elsevier.com/locate/bmcl

Total synthesis and evaluation of C25-benzyloxyepothilone C for tubulin assembly and cytotoxicity against MCF-7 breast cancer cells

Oliver E. Hutt [a], Bollu S. Reddy [a], Sajiv K. Nair [a], Emily A. Reiff [a], John T. Henri [a], Jack F. Greiner [a], Ting-Lan Chiu [c], David G. VanderVelde [a], Elizabeth A. Amin [c], Richard H. Himes [b], Gunda I. Georg [a,c,*]

[a] Department of Medicinal Chemistry, University of Kansas, 1251 Wescoe Hall Drive, Lawrence, KS 66045, USA
[b] Department of Molecular Bioscience, University of Kansas, 1200 Sunnyside Avenue, Lawrence, KS 66045, USA
[c] Department of Medicinal Chemistry, and Institute for Therapeutics Discovery and Development, University of Minnesota, 717 Delaware Street SE, Minneapolis, MN 55414, USA

ARTICLE INFO

Article history:
Received 6 May 2008
Accepted 1 July 2008
Available online 11 July 2008

Keywords:
Epothilones
C-25 epothilone analogue
Total synthesis
Tubulin assembly
Cytotoxicity

ABSTRACT

The total synthesis of C25-benzyloxy epothilone C is described. A sequential Suzuki–Aldol–Yamaguchi macrolactonization strategy was utilized employing a novel derivatized C8–C12 fragment. The C25-benzyloxy analog exhibited significantly reduced biological activity in microtubule assembly and cytotoxicity assays. Molecular modeling simulations indicated that excessive steric bulk in the C25 position may reduce activity by disrupting key hydrogen bonds that are crucial for epothilone binding to β-tubulin.

The epothilone class of natural products is a family of potent cytotoxic polyketide marcolides first isolated in 1992 by Höfle et al. from the myxobacterium *Sorangium cellulosum*.[1,2] Like paclitaxel, they disrupt microtubule dynamics, resulting in cell cycle arrest and apoptosis.[3,4] Most importantly, the epothilones maintain impressive efficacy against several paclitaxel-resistant cancer cell lines and they are now generally recognized as the next generation of clinically relevant anti-mitotic agents. Some members of the epothilone family contain an epoxide while others, typified by epothilone C (**1**) and epothilone D (**2**), contain a double bond in place of the epoxide moiety (Fig. 1).

Resistance to paclitaxel has arisen through three main mechanisms: overexpression of P-glycoprotein (Pgp), which lowers the intracellular concentration of the drug, overexpression of the β-tubulin isotype β-III, and tubulin point-mutations in key amino acid residues important to taxane binding.[5] The epothilones appear to be able to evade Pgp efflux and retain activity in cell lines that have become resistant to paclitaxel because of mutations in β-tubulin. This implies that, despite sharing a common binding site on β-tubulin, the mode of binding of paclitaxel and the epothilones is significantly different.[6] As a result, early attempts to find a shared pharmacophore between paclitaxel and epothilone B were unsuccessful.[7–10] The clinical importance of this class of compounds has led to an explosion of synthetic activity[7] and structural studies have led to two β-tubulin-epothilone binding models. The first is based on electron crystallography (EC) of Zn^{2+} induced tubulin sheets,[11] while the second is derived from NMR studies.[12]

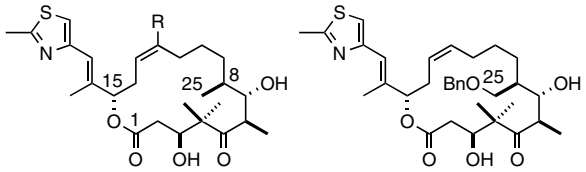

1 R = H epothilone C
2 R = Me epothilone D

3

Figure 1. Structures of epothilones.

One approach to gaining supporting evidence for either of these binding hypotheses is through photoaffinity labeling of microtubules with an appropriate photoreactive epothilone analog. Toward this end we have synthesized the C25-benzyloxy derivative **3** (Fig. 1) as a potential precursor to a photoaffinity analog. We now report the synthesis of **3** and the resulting microtubule assembly and cytotoxicity studies.

The synthetic strategy for the synthesis of **3** is outlined in Figure 2 and involved the preparation and successive coupling of building blocks **4**, **5**, and **6**.[13,14] We envisioned that the C11–C12 bond would be formed by a Suzuki reaction, the C6–C7 bond by an Aldol reaction, and the use of the Yamaguchi procedure to form the macrocycle.

* Corresponding author. Tel.: +1 785 864 4498; fax: +1 785 864 5836.
E-mail address: georg239@umn.edu (G.I. Georg).

0960-894X/$ - see front matter © 2008 Published by Elsevier Ltd.
doi:10.1016/j.bmcl.2008.07.024

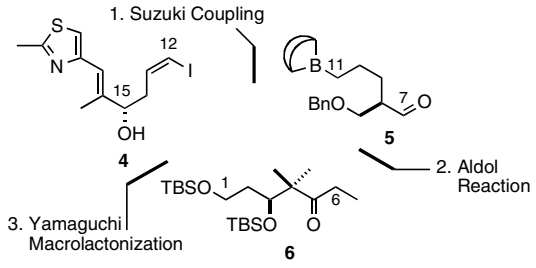

Figure 2. Synthetic strategy for the construction of **3**.

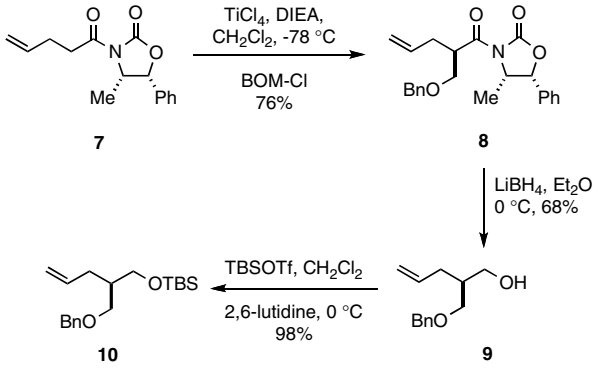

Scheme 1. Synthesis of fragment **10**.

Fragments **4** and **6** were synthesized as previously reported.[15] The synthesis of the precursor to fragment **5** is outlined in Scheme 1.[16] The oxazolidinone **7** was readily obtained through the acylation of the oxazolidinone core with pent-4-enoyl chloride. The C8 stereochemistry was then established through alkylation of **7** with BOM–Cl to furnish benzyloxy intermediate **8** in 76% yield. The auxiliary was then reductively cleaved on treatment of **8** with $LiBH_4$ to provide alcohol **9** in 68% yield. The alcohol moiety of **9** was subsequently protected as the TBS ether **10** in preparation for the planned Suzuki coupling (Scheme 2).

With fragment **10** in hand the synthesis of **3** was accomplished as shown in Scheme 2. The alkene function of **10** was subjected to hydroboration with 9-BBN, and the ensuing Sukuzi coupling with vinyl iodide **4** delivered the desired cis alkene **11** in 92% yield.

The primary TBS ether functionality of **11** was then selectively cleaved in 82% yield on treatment with fluorosilicic acid (H_2SiF_6),[14,17] and the resulting alcohol was subsequently oxidized with 2-iodoxybenzoic acid (IBX) in EtOAc to give the aldehyde **12** in 95% yield. The stage was now set to install the final fragment. Accordingly, ketone **6** was treated with LDA to generate the *Z*-enolate, which was subsequently treated with aldehyde **12** to deliver the syn-Aldol product **13** in 54% yield.

The secondary alcohol function of **13** was protected as the TBS ether. The primary TBS ether was then selectively deprotected (84% yield) with fluorosilicic acid, and the resulting alcohol was sequentially oxidized with Dess–Martin periodane (DMP) and perchlorate to the C1 acid in preparation for the Yamaguchi macrolactonization.

The allylic alcohol group at C15 was deprotected and the subsequent Yamaguchi macrolactonization delivered the core epothilone skeleton **14**. Deprotection of the TBS groups furnished the target compound **3** (Scheme 2).

With the desired probe in hand we could begin to test its suitability for biological studies. As the two most commonly used photoaffinity labels are aryl azide and aryl diazirines, the steric demand of the benzyl function of **3** would serve as an acceptable surrogate to probe the suitability of this approach.[18] Unfortunately, at a concentration of 100 μM, compound **3** was completely inactive in a microtubule assembly assay (EC_{50} for epothilone $B = 2.5$ μM)[19] and was essentially devoid of cytotoxicity against the cancer cell line MCF-7 (2.1 μM, $ED_{50}/ED_{50Epo\ B} = 1050$).[19] The available evidence suggests that the loss of activity is not due to a change in the solution conformation of the free compound, but to an unfavorable interaction in the bound form. Comparison of the solution NMR data of **3** with epothilone A,[20] the C12–C13 β-epoxide of epothilone C (**1**) indicates there are only local and relatively small conformational adjustments to the steric demand of the OBn group: the H6–H7 coupling constant declined from 9 Hz to 7 Hz. This represents a change in the torsion angle of approximately 15 degrees. Thus, both the C8 methyl group of the parent compound and the OBn group in **3** essentially point away from the macrocycle and toward a hydrophobic surface of the protein in the models of the bound state. These data suggested that the OBn group was too large to fit into this sterically constrained hydrophobic area.

To probe this hypothesis a molecular modeling study was conducted. The pre-docked conformation of C25-benzyloxyepothilone C was first prepared by modifying the experimental EpoA structure and optimizing the resulting geometry using the MMFF94s force field in MOE (Chemical Computing Group, Inc.). The optimized

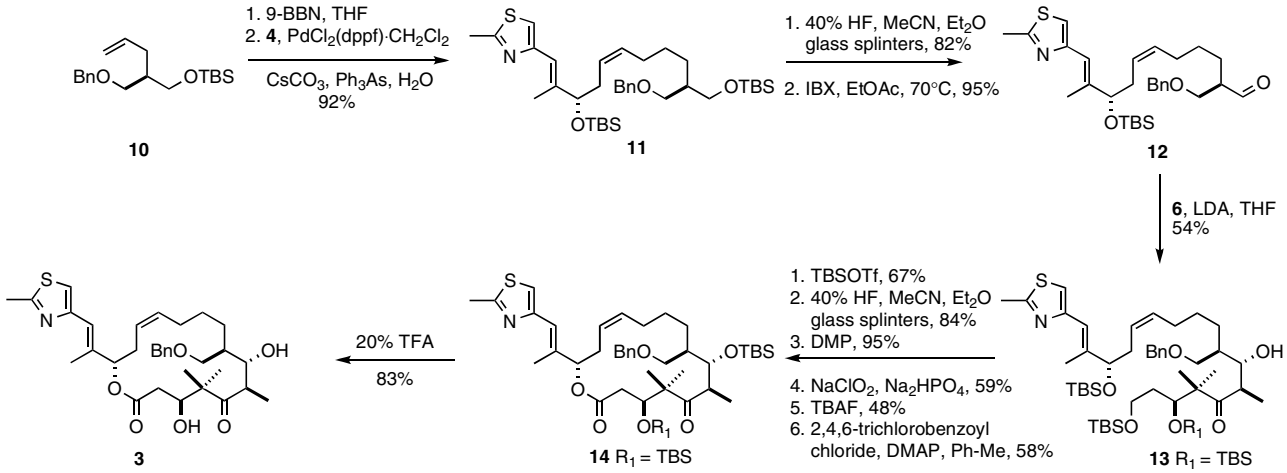

Scheme 2. Synthesis of target compound **3**.

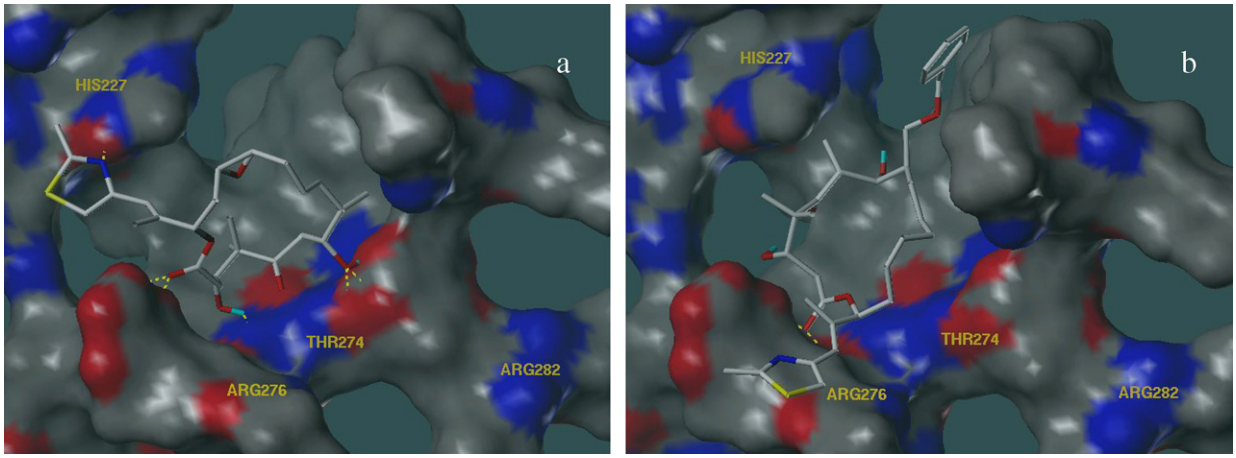

Figure 3. Docked configurations (Surflex-Dock, Tripos, Inc.) of epothilone A (a, left panel) and C25-benzyloxyepothilone C (b, right panel) are shown with MOLCAD (Tripos, Inc.) electron density surfaces of the tubulin binding site (1TVK[11]), onto which hydrogen bond donor and acceptor regions have been mapped. Red areas represent hydrogen bond donors; blue areas represent hydrogen bond acceptors; and gray indicates regions in which no hydrogen bonding takes place. Key ligand–receptor interactions are shown in both pictures. In (a), hydrogen bonding occurs between the EpoA thiazole nitrogen and the imidazole NH of His227; between the EpoA C1 carbonyl and two amino groups in Arg276; between the EpoA C3 hydroxyl and the Thr274 backbone carbonyl; between the EpoA C5 carbonyl and the Thr274 backbone NH; and between the EpoA C7 OH and Arg282 and Pro272. In the docked configuration of C25-benzyloxyepothilone C (b), all of these interactions disappear due to sterically driven ligand rearrangement, except for a single hydrogen bond between the epothilone C1 carbonyl and Arg276. Validation was performed by comparing the docked configuration of EpoA to the experiment (RMSD = 1.575 Å).

C25-benzyloxyepothilone C used for docking was in good agreement with the predicted solution conformation of EpoA and with the NMR experimental results. When the C25-benzyloxy analog was docked into the tubulin binding site (Fig. 3), as predicted, the OBn group proved too large. The subsequent reorientation of the molecule in the binding site disrupted two crucial hydrogen-bonding interactions: between the thiazole nitrogen and the imidazole NH of His227 and between the C7–OH and Arg282 and Pro272.

In conclusion, we have synthesized the first C25 functionalized epothilone derivative[21] as a model to test the suitability of this position for the placement of a photoreactive function. Unfortunately, this analog was inactive due to the steric demand at the C25 position, which disabled key hydrogen bonds resulting in significantly weaker ligand binding.

Acknowledgment

The authors gratefully acknowledge financial support from the National Institutes of Health: National Cancer Institute CA79641.

References and notes

1. Höfle, G.; Bedorf, N.; Gerth, K.; Reichenbach, H. *Offenlegungsschrift der Bundesrepublik Deutschland* **1993**, *DE 4138042*, A1.
2. Gerth, K.; Bedorf, N.; Hoefle, G.; Irschik, H.; Reichenbach, H. *J. Antibiot.* **1996**, *49*, 560.
3. Bollag, D. M.; McQueney, P. A.; Zhu, J.; Hensens, O.; Koupal, L.; Liesch, J.; Goetz, M.; Lazarides, E.; Woods, C. M. *Cancer Res.* **1995**, *55*, 2325.
4. Altmann, K.-H. *Curr. Pharm. Des.* **2005**, *11*, 1595.
5. Fojo, T.; Menefee, M. *Ann. Oncol.* **2007**, *18*, v3.
6. Gupta, M. L., Jr.; Bode, C. J.; Georg, G. I.; Himes, R. H. *Proc. Natl. Acad. Sci. U.S.A.* **2003**, *100*, 6394.
7. Wang, M.; Xia, X.; Kim, Y.; Hwang, D.; Jansen, J. M.; Botta, M.; Liotta, D. C.; Snyder, J. P. *Org. Lett.* **1999**, *1*, 43.
8. Ojima, I.; Chakravarty, S.; Inoue, T.; Lin, S.; He, L.; Horwitz, S. B.; Kuduk, S. D.; Danishefsky, S. J. *Proc. Natl. Acad. Sci. U.S.A.* **1999**, *96*, 4256.
9. He, L.; Jagtap, P. G.; Kingston, D. G. I.; Shen, H.-J.; Orr, G. A.; Horwitz, S. B. *Biochemistry* **2000**, *39*, 3972.
10. Giannakakou, P.; Gussio, R.; Nogales, E.; Downing, K. H.; Zaharevitz, D.; Bollbuck, B.; Poy, G.; Sackett, D.; Nicolaou, K. C.; Fojo, T. *Proc. Natl. Acad. Sci. U.S.A.* **2000**, *97*, 2904.
11. Nettles, J. H.; Li, H.; Cornett, B.; Krahn Joseph, M.; Snyder James, P.; Downing Kenneth, H. *Science* **2004**, *305*, 866.
12. Reese, M.; Sanchez-Pedregal, V. M.; Kubicek, K.; Meiler, J.; Blommers, M. J. J.; Griesinger, C.; Carlomagno, T. *Angew. Chem., Int. Ed.* **2007**, *46*, 1864.
13. Balog, A.; Meng, D.; Kamenecka, T.; Bertinato, P.; Su, D.-S.; Sorensen, E. J.; Danishefsky, S. J. *Angew. Chem., Int. Ed.* **1997**, *35*, 2801.
14. Schinzer, D.; Bauer, A.; Schieber, J. *Chem. Eur. J.* **1999**, *5*, 2492.
15. Reiff, E. A.; Nair, S. K.; Reddy, B. S. N.; Inagaki, J.; Henri, J. T.; Greiner, J. F.; Georg, G. I. *Tetrahedron Lett.* **2004**, *45*, 5845.
16. Evans, D. A.; Urpi, F.; Somers, T. C.; Clark, J. S.; Bilodeau, M. T. *J. Am. Chem. Soc.* **1990**, *112*, 8215.
17. Pilcher, A. S.; DeShong, P. *J. Org. Chem.* **1993**, *58*, 5130.
18. Dorman, G.; Prestwich, G. D. *Trends Biotechnol.* **2000**, *18*, 64.
19. Liu, Y.; Ali, S. M.; Boge, T. C.; Georg, G. I.; Victory, S.; Zygmunt, J.; Marquez, R. T.; Himes, R. H. *Comb. Chem. High Throughput Screening* **2002**, *5*, 39.
20. Victory, S. F.; Vander Velde, D. G.; Jalluri, R. K.; Grunewald, G. L.; Georg, G. I. *Bioorg. Med. Chem. Lett.* **1996**, *6*, 893.
21. The spectroscopic data of all intermediates were in agreement with their structures. Spectroscopic data for compound **3**: ^{1}H NMR (400 MHz, $CDCl_3$) δ 7.37–7.29 (m, 5H), 6.97 (s, 1H), 6.56 (s, 1H), 5.47 (m 1H), 5.37 (m, 1H), 5.24 (d, J = 7.8 Hz, 1H), 4.55 (d, J = 11.9 Hz, 1H), 4.47 (d, J = 11.0 Hz, 1H), 4.04 (obscured br d, J = 7.0 Hz, 1H), 4.01 (m, 1H), 3.63 (dd, J = 2.9 Hz, J = 9.2 Hz, 1H), 3.57 (dd, J = 3.6 Hz, J = 9.2 Hz, 1H), 3.23 (s, 1H), 3.18 (t, J = 6.9 Hz, 1H), 2.70 (s and obscured m, 4H), 2.51 (d, J = 2.8 Hz, 2H), 2.49 (s, 1H), 2.22–2.15 (m, 2H), 2.10 (s, 3H), 1.98–1.90 (m, 1H), 1.70–1.50 (m, 4H), 1.35 (m, 1H), 1.31 (s, 3H), 1.20 (d, J = 6.8 Hz, 3H), 1.11 (s, 3H); ^{13}C NMR (100 MHz, $CDCl_3$) δ 218.8, 170.7, 164.9, 152.1, 138.0, 137.9, 133.9, 128.4, 127.7, 127.6, 123.9, 119.8, 116.2, 78.9, 75.73, 73.4, 73.4, 72.0, 52.4, 45.1, 41.8, 38.7, 31.4, 28.3, 27.8, 25.2, 21.9, 21.8, 19.2, 15.4, 15.4; MS (FAB) m/e 584.4 (M+H); $[\alpha]_D^{20} - 23$ (c 0.29, $CHCl_3$).